Supporting information for

Low thermal conductivity in Si/Ge hetero-twinned superlattices

Huicong Dong[a], Bin Wen [a 1], Yuwen Zhang[b], Roderick Melnik[c]

[a] State Key Laboratory of Metastable Materials Science and Technology, Yanshan University, Qinhuangdao 066004, China

[b] Department of Mechanical and Aerospace Engineering, University of Missouri-Columbia, Columbia, Missouri, USA

[c] The MS2Discovery Interdisciplinary Research Institute, Wilfrid Laurier University, 75 University Ave. West, Waterloo, Ontario, Canada N2L 3C5

This file includes:

Discussion 1: Thermal conductivity calculation by non-equilibrium molecular dynamic simulations

Discussion 2: Interface thermal resistance calculation by NEMD simulation

Discussion 3: Heat capacity calculation by quasiharmonic approximation (QHA) theory

Figure S1 Linear relationship between the inverse of model length and the inverse of thermal conductivity.

Figure S2 Thermal conductivity calculation by NEMD simulation. (a) A model used for NEMD simulation, the hot region is placed in the middle, and the cold regions are placed at the ends. (b) Calculated temperature profile along the thermal transmission direction.

Figure S3 Model length dependent temperature profiles for Si/Ge hetero-twinned SLs with a periodic thickness of 7.7 nm, the model length ranges from 15.4 nm to 53.88 nm.

[a 1] Authors to whom any correspondence should be addressed

E-mail address: wenbin@ysu.edu.cn (Bin Wen), Tel: 086-335-8568761

Figure S4 Comparison of phonon dispersions for Si/Ge hetero-twinned SLs, single crystal Si, twinned Si, $Si_{0.5}Ge_{0.5}$ alloys and conventional Si/Ge SLs. Only the acoustic branches are shown, "TA1", "TA2" and "LA" correspond to two transverse branches and one longitudinal branch. "Si" corresponds to single Si crystal, "Twinned Si" corresponds to twinned Si crystal, "Alloy" corresponds to $Si_{0.5}Ge_{0.5}$ alloy, "Con-SLs" corresponds to conventional Si/Ge SLs, and "Hete-TB SLs" corresponds to Si/Ge hetero-twinned SLs.

Figure S5 Comparison of phase velocities for Si/Ge hetero-twinned SLs, single crystal Si, twinned Si, $Si_{0.5}Ge_{0.5}$ alloys and conventional Si/Ge SLs. Only the acoustic branches are shown, "TA1", "TA2" and "LA" correspond to two transverse branches and one longitudinal branch. "Si" corresponds to single Si crystal, "Twinned Si" corresponds to twinned Si crystal, "Alloy" corresponds to $Si_{0.5}Ge_{0.5}$ alloy, "Con-SLs" corresponds to conventional Si/Ge SLs, and "Hete-TB SLs" corresponds to Si/Ge hetero-twinned SLs.

Figure S6 Comparison of Grüneisen parameters for Si/Ge hetero-twinned SLs, single crystal Si, twinned Si, $Si_{0.5}Ge_{0.5}$ alloys and conventional Si/Ge SLs. Only the acoustic branches are shown, "TA1", "TA2" and "LA" correspond to two transverse branches and one longitudinal branch. "Si" corresponds to single Si crystal, "Twinned Si" corresponds to twinned Si crystal, "Alloy" corresponds to $Si_{0.5}Ge_{0.5}$ alloy, "Con-SLs" corresponds to conventional Si/Ge SLs, and "Hete-TB SLs" corresponds to Si/Ge hetero-twinned SLs.

Discussion 1: Thermal conductivity calculation by non-equilibrium molecular dynamic simulations

Thermal conductivities of Si/Ge hetero-twinned SLs, as well as that of bulk single crystal Si, twinned Si, $Si_{0.5}Ge_{0.5}$ alloy, and conventional Si/Ge SLs along [111] are calculated by non-equilibrium molecular dynamic (NEMD) simulations[1, 2], which have been carried out by imposing a heat flux on the simulation system to obtain a temperature gradient[3]. As can be seen in Figure S2 (a), the hot region is placed in the middle, and the cold regions are at the ends of the simulation system. As a result, the heat flux can be imposed by exchanging the velocities of the hottest atoms in the cold region with the coldest atoms in the hot region, which can be described by[3]

$$J = \frac{1}{2tA}\sum_{transfer}\frac{m}{2}(v_{hot}^2 - v_{cold}^2), \quad (1)$$

where t is the simulation time, A is the cross-sectional area of the simulation system perpendicular to the direction of the heat flux, m is the atom mass, v_{hot} and v_{cold} denote the velocities of the hottest and coldest atoms to be exchanged at each step, and the factor 2 arises from the periodicity. When the heat transmission reaches to a steady state, the thermal conductivity can be obtained from the relationship between the heat flux and temperature gradient as shown in Figure S2 (b) by applying the Fourier's heat conduction law[3]

$$J = -KdT / dx, \quad (2)$$

where K is the thermal conductivity, dT/dx is the temperature gradient averaged over time and space, and J is the heat flux density, which is given by the sum of exchanged energy per unit time and area.

Discussion 2: Interface thermal resistance calculation by NEMD simulation

To obtain the interface thermal resistance, NEMD simulations[2, 4] are carried out. Interface thermal resistance R_K is defined as the ratio of temperature jump ΔT at the interface by the heat flux J passing through it, as shown in the following[5]

$$R_K = \frac{\Delta T}{J} \tag{3}$$

Figure S3 shows the model length dependent temperature profiles for Si/Ge hetero-twinned SLs with a periodic thickness of 7.7 nm, the model length in simulation ranges from 15.4 nm to 53.88 nm. It can be seen that with the increase of model length, the temperature jumps at the interfaces are decreased. Moreover, it can also be observed that at the ends of model length, the temperature jump is extremely large due to the effect of boundary. Interface thermal resistance can be calculated by applying Eq. (3), and to eliminate the boundary effect, only temperature jumps in the middle part of model are used.

Discussion 3: Heat capacity calculation by quasiharmonic approximation (QHA) theory

In this work, the heat capacity of Si/Ge hetero-twinned SLs, as well as the heat capacities of bulk single crystal Si, twinned Si, $Si_{0.5}Ge_{0.5}$ alloy, and conventional Si/Ge SLs are calculated by using the density functional theory combined with the quasiharmonic approximation (DFT-QHA) theory[6]. The heat capacity[7] can be expressed as

$$C = \sum_{n,\mathbf{q}} k_B \left(\frac{\hbar\omega_n(\mathbf{q})}{k_B T}\right)^2 \frac{e^{\hbar\omega_n(\mathbf{q})} / k_B T}{(e^{\hbar\omega_n(\mathbf{q})/k_B T} - 1)^2}, \quad (4)$$

where $\hbar$ is the Planck constant, k_B is the Boltzmann constant, T is the temperature, and $\omega_n(\mathbf{q})$ is the phonon frequency of the n-th branch with wave vector $\mathbf{q}$.

Heat capacity calculations are performed by implementing the Vienna Ab initio Simulation Package (VASP)[8], which employs the plane-wave basis. Phonon dispersions in the five structures are calculated by using the supercell approach with the finite displacement method implemented in the PHONOPY package[8] . The plane-wave energy cutoff has been set to be 500 eV, and the electronic energy convergence is 10^{-6} eV. In structure relaxations, the force convergence has been set to be 10^{-3}eV/A. In phonon calculations, supercells for the five structures all contain 24 atoms, and a Γ-centered $4\times6\times3$ Monkhorst-Pack k-point mesh is used to sample the irreducible Brillouin zone.

References

1. C. Oligschleger and J. C. Schön, *Phys. Rev. B*, 1999, **59**, 4125.
2. F. Müller-Plathe, *J. Chem. Phys.*, 1997, **106**, 6082.
3. A. Bagri, S.-P. Kim, R. S. Ruoff and V. B. Shenoy, *Nano Lett.*, 2011, **11**, 3917-3921.
4. D. R. F. Müller-Plathe, *Comput. Theor. Polym. Sci.*, 1999, **9**, 203-209.
5. J. P. Crocombette and L. Gelebart, *J. Appl. Phys.*, 2009, **106**, 083520.
6. A. Otero-de-la-Roza and V. Luaña, *Phys. Rev. B*, 2011, **84**, 184103.
7. H. Shao, X. Tan, T. Hu, G.-Q. Liu, J. Jiang and H. Jiang, *EPL*, 2015, **109**, 47004.
8. G. Kresse and J. Hafner, *Phys. Rev. B*, 1993, **47**, 558-561.

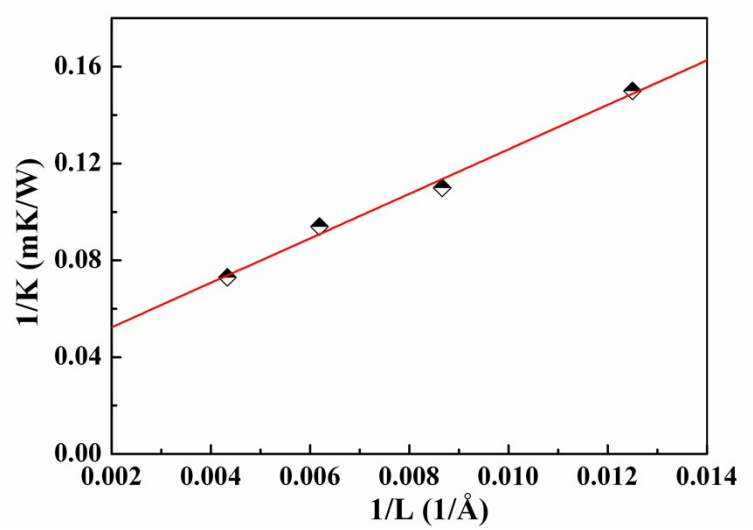

Figure S1 Linear relationship between the inverse of model length and the inverse of thermal conductivity.

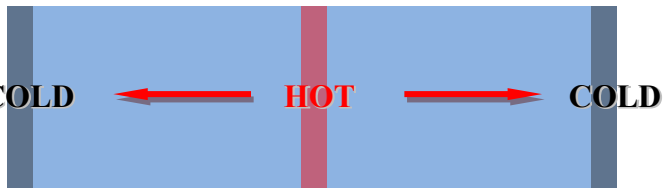

(a)

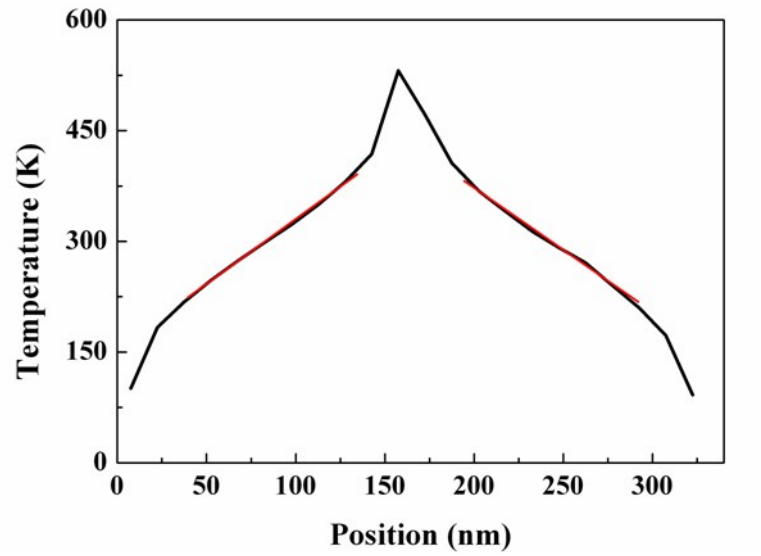

(b)

Figure S2 Thermal conductivity calculation by NEMD simulation. (a) A model used for NEMD simulation, the hot region is placed in the middle, and the cold regions are placed at the ends. (b) Calculated temperature profile along the thermal transmission direction.

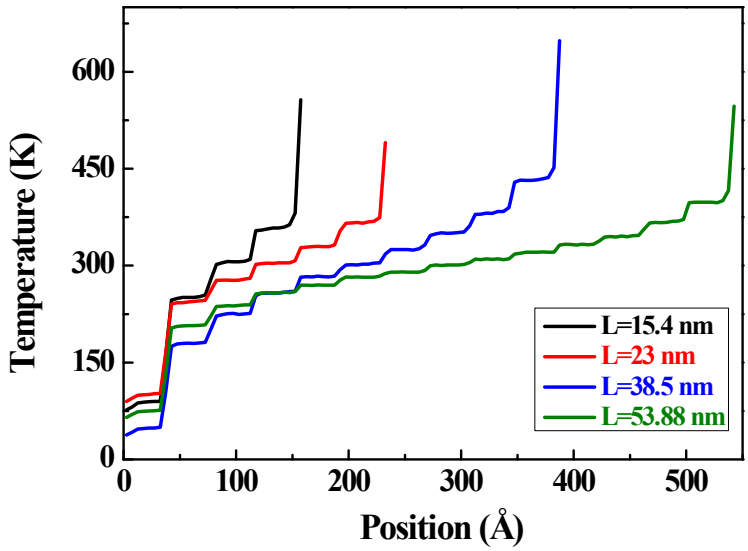

Figure S3 Model length dependent temperature profiles for Si/Ge hetero-twinned SLs with a periodic thickness of 7.7 nm, the model length ranges from 15.4 nm to 53.88 nm.

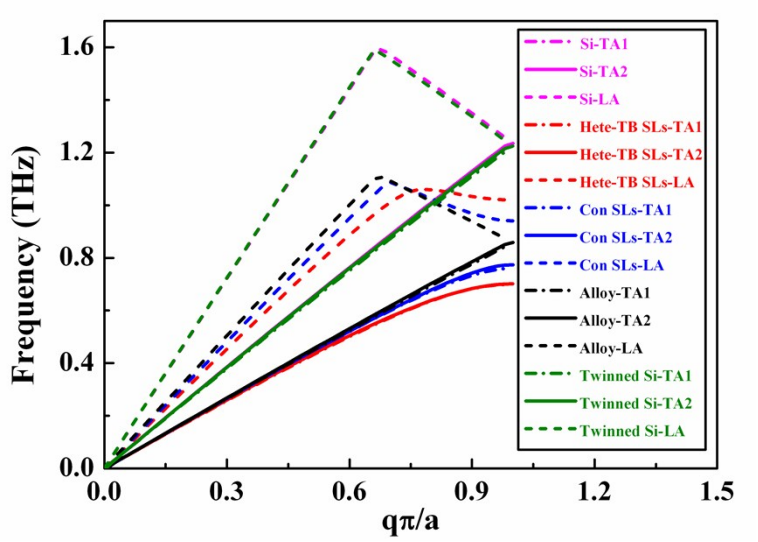

Figure S4 Comparison of phonon dispersions for Si/Ge hetero-twinned SLs, single crystal Si, twinned Si, $Si_{0.5}Ge_{0.5}$ alloys and conventional Si/Ge SLs. Only the acoustic branches are shown, "TA1", "TA2" and "LA" correspond to two transverse branches and one longitudinal branch. "Si" corresponds to single Si crystal, "Twinned Si" corresponds to twinned Si crystal, "Alloy" corresponds to $Si_{0.5}Ge_{0.5}$ alloy, "Con-SLs" corresponds to conventional Si/Ge SLs, and "Hete-TB SLs" corresponds to Si/Ge hetero-twinned SLs.

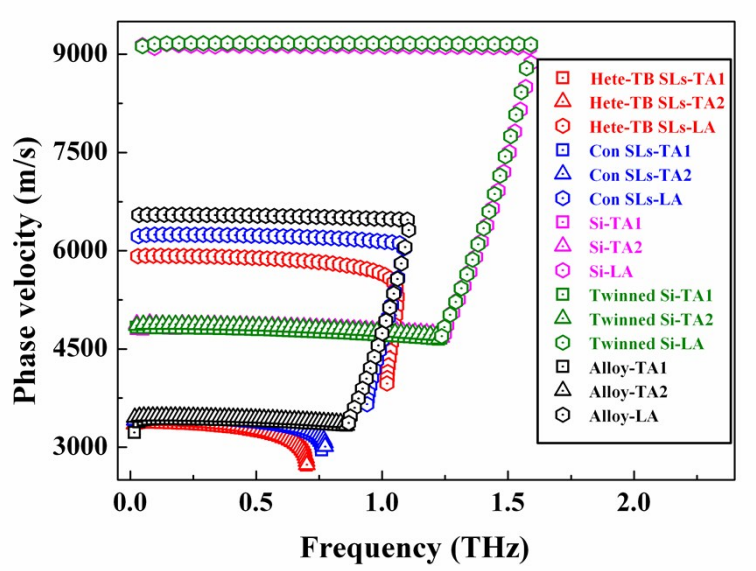

Figure S5 Comparison of phase velocities for Si/Ge hetero-twinned SLs, single crystal Si, twinned Si, $Si_{0.5}Ge_{0.5}$ alloys and conventional Si/Ge SLs. Only the acoustic branches are shown, "TA1", "TA2" and "LA" correspond to two transverse branches and one longitudinal branch. "Si" corresponds to single Si crystal, "Twinned Si" corresponds to twinned Si crystal, "Alloy" corresponds to $Si_{0.5}Ge_{0.5}$ alloy, "Con-SLs" corresponds to conventional Si/Ge SLs, and "Hete-TB SLs" corresponds to Si/Ge hetero-twinned SLs.

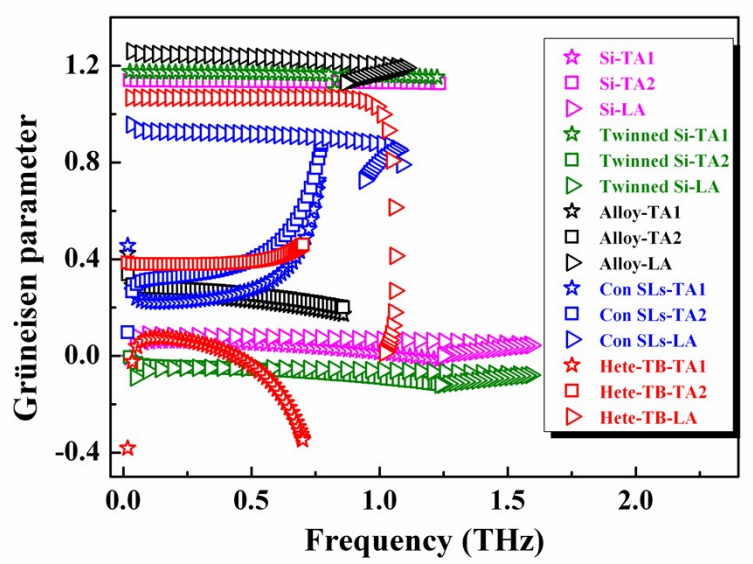

Figure S6 Comparison of Grüneisen parameters for Si/Ge hetero-twinned SLs, single crystal Si, twinned Si, $Si_{0.5}Ge_{0.5}$ alloys and conventional Si/Ge SLs. Only the acoustic branches are shown, "TA1", "TA2" and "LA" corresponds two transverse branches and one longitudinal branch. "Si" corresponds to single Si crystal, "Twinned Si" corresponds to twinned Si crystal, "Alloy" corresponds to $Si_{0.5}Ge_{0.5}$ alloy, "Con-SLs" corresponds to conventional Si/Ge SLs, and "Hete-TB SLs" corresponds to Si/Ge hetero-twinned SLs.